Earth Planet. Sci. Lett. 646 (2024) 119008

Contents lists available at ScienceDirect

Earth and Planetary Science Letters

journal homepage: www.elsevier.com/locate/epsl

Earth-Moon refractory element similarity constrains a thoroughly-mixed Moon-forming disk

Hairuo Fu *, Stein B. Jacobsen

Department of Earth and Planetary Sciences, Harvard University, Cambridge, MA 02138, USA

ARTICLE INFO

Editor: Olivier Mousis

ABSTRACT

The canonical Moon-forming giant-impact models allow for substantial chemical differences between the bulk silicate Moon and Earth due to incomplete mixing of the impactor and the proto-Earth. In comparison, the emerging high-energy giant-impact (Synestia) model requires the refractory element compositions of the Earth and Moon to be nearly identical, owing to extensive chemical homogenization of the Moon-forming disk in a vigorously mixed silicate fluid. These distinct chemical predictions make the lunar refractory element composition crucial for testing Moon-formation hypotheses, yet it remains highly controversial and necessitates new approaches to resolve. In this study, we develop a novel method using the composition of pristine lunar anorthosite samples to constrain the Moon's refractory lithophile element compositions. We obtained a very close match of refractory major and trace element compositions for the lunar magma ocean model, suggesting indistinguishable refractory element abundances between the bulk silicate Moon and Earth. This striking refractory element similarity is difficult to reconcile with the relatively poor mixing conditions of the canonical giant-impact models. The compatibility of this result with disk equilibration models other than the Synestia has yet to be quantitatively verified. Our results further constrain that the formation of the Earth-Moon system requires a thoroughly-mixed protolunar disk of chemical and isotopic homogenization with an initially fully-molten Moon, as enabled by emerging models like the Synestia.

1. Introduction

The bulk chemical composition of the Moon is fundamental to understanding the formation of the Earth-Moon system. In particular, the refractory lithophile elements [with high equilibrium condensation temperatures such as Ca, Al, Sr, Th, and rare earth elements (REEs)] carry unparalleled significance because their compositions are representative of the Moon's primitive building materials, in contrast to the volatile and siderophile elements and their isotopes that can be further modified by planetary accretion and core segregation.

Over the past years, extensive efforts and progress have been made on understanding the importance of the observed similar Earth-Moon mass-independent isotope signatures in testing Moon-forming giant-impact models, such as the $\Delta^{17}O$ (Young et al., 2016), $\varepsilon^{50}Ti$ (Zhang et al., 2012), and $\varepsilon^{54}Cr$ compositions (Qin et al., 2010; Mougel et al., 2018). However, the significance of refractory elements and their mass-dependent isotopic fractionation (e.g., $\delta^{44/40}Ca$ and $\delta^{49/47}Ti$) of the Earth-Moon system has yet to be adequately explored. These element and isotopic proxies differ fundamentally from mass-independent isotope systematics in that their variations are subject to internal planetary differentiation and were likely heterogeneous across the Moon-forming impactor and proto-Earth. In contrast, the mass-independent isotopic composition (e.g., $\Delta^{17}O$, $\varepsilon^{50}Ti$, $\varepsilon^{54}Cr$) is mostly uniform in the mantle of each body. The variable nature of the refractory elements and their isotopic fractionation in the pre-impact bodies could principally place stronger constraints on the details of giant-impact mixing processes. Additionally, the refractory elements and their isotopes are most resistant to evaporation and mixing, thereby yielding more restrictive limits on the required extent of protolunar disk mixing than volatile elements. These unique advantages should motivate a new generation of Moon-formation testing by leveraging this underexplored element and isotopic array.

In the canonical (low-energy) giant-impact hypothesis for the Moon's formation (e.g., Canup, 2004; Kegerreis et al., 2022; Canup et al., 2023;), the Mars-sized impactor (Theia) and the proto-Earth are considered to be differentiated bodies that likely hold mantle chemical

* Corresponding author.
E-mail address: hairuo.fu@g.harvard.edu (H. Fu).

https://doi.org/10.1016/j.epsl.2024.119008
Received 24 June 2024; Received in revised form 12 August 2024; Accepted 10 September 2024
Available online 18 September 2024

heterogeneities in element ratio and concentration, set by early magma ocean compositional differentiation (Elkins-Tanton, 2012). The bulk silicate Moon (BSM) is made from sampling minor portions of the mantles of both bodies, preferentially from their outer portions, a phenomenon known as the "shallow-province bias" (Warren, 2005). Meanwhile, the majority of the remaining silicate materials form the bulk silicate Earth (BSE) (Fig. 1). In these models, we find it difficult for the BSM to sample the average chemical composition of the combined silicate portions of the two bodies. This difficulty arises from two main factors. First, the outer silicate portions of the two bodies are likely chemically heterogeneous and not representative of the average mantle compositions. Therefore, their preferential sampling into the disk would likely result in a chemically fractionated BSM composition from the BSE. Second, the BSM samples only a minimal mass fraction (~2 %) of the total silicate materials, leaving most of Theia and proto-Earth materials unmixed in the Moon-forming disk. Given the biased sampling and poor disk-mixing characteristics, in the canonical giant-impact models, the BSM is likely distinct from the BSE in refractory element ratio and concentration (Fig. 1).

This predicted chemical discrepancy can be substantial regardless of whether (i) Theia and the proto-Earth shared similar bulk compositions or (ii) how much materials the BSM sources derived from Theia versus the proto-Earth (including the scenarios in which BSM sources solely from Theia or the proto-Earth). This prediction is due to the BSM sampling such minimal mass fractions from either body, which both likely carried planetary-scale chemical heterogeneities. Likewise, different BSM and BSE refractory element compositions should also be expected in the canonical models where Theia is similar in size to the proto-Earth, instead of being Mars-sized (Canup, 2012).

Other modified giant-impact models also allow for substantial chemical differences between the Earth and the Moon. For example, the disk equilibration hypothesis of the Moon's formation (Pahlevan and Stevenson, 2007), which was proposed to explain the observed identical oxygen isotope signatures, was found challenging to effectively homogenize refractory elements and their isotopes due to their much higher condensation temperatures and resistance to evaporation and turbulent mixing (Zindler and Jacobsen, 2010; Zhang et al., 2012; Melosh, 2014). Moreover, Hosono et al. (2019) proposed a model where the Moon's building materials are sourced mostly from a terrestrial magma ocean, attempting to reconcile the isotopic similarity of the Earth-Moon system. However, we find that such models also predict and allow for a significant compositional difference between the Earth and Moon. Despite assuming an ideal, chemically-homogenized terrestrial magma ocean covering the Earth's deeper mantle, this shallow magma ocean is likely chemically fractionated from the underlying mantle and the BSE due to solid-melt refractory element partitioning during the early magma ocean crystallization or partial melting of the pre-existing mantle. This chemically fractionated terrestrial magma ocean, which later forms the primary composition of the Moon in this model, is expected to be chemically distinct from the BSE. Other protolunar disk models, which propose improved disk mixing conditions due to the potential magnetorotational instability (MRI) driven turbulence (e.g., Charnoz and Michaut, 2015; Gammie et al., 2016), remain unclear about the mixing efficacy for refractory elements. As a result, a predicted Earth-Moon refractory element composition is currently unavailable in such models, preventing a direct comparison with the observations.

In contrast, the recent Earth-Moon Synestia model (Lock et al., 2018), where the BSM condenses out of a homogenized BSE fluid due to a high-energy, high-angular-momentum impact (Fig. 1), requires an initially fully molten Moon and the BSM and BSE chemical compositions to be close to identical in refractory elements (~2.7 times CI chondrite) (McDonough and Sun, 1995). Given the contrasting Earth-Moon

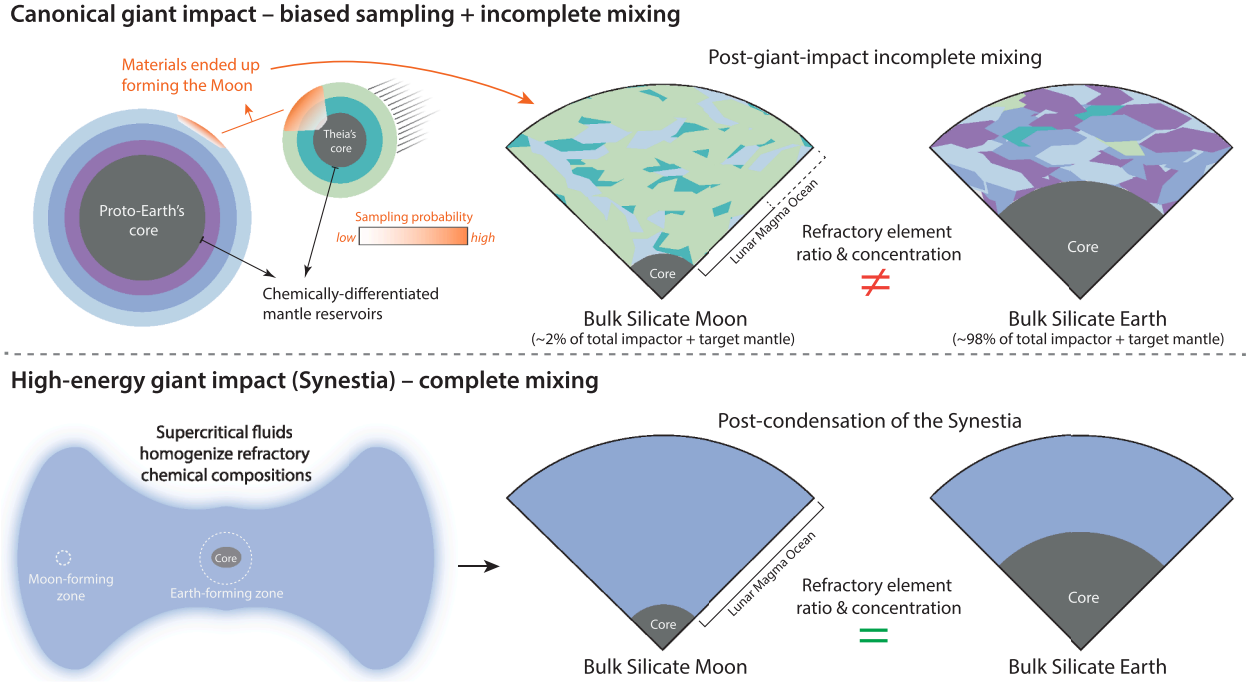

Fig. 1. Silicate Earth's and Moon's chemical building blocks and compositions expected for various Moon-forming mechanisms. In the upper panel, the canonical low-energy giant-impact scenarios (Canup et al., 2023) predict the Moon being made from small portions of chemically and isotopically fractionated materials sampled from the impactor (Theia) and the proto-Earth. In particular, the Moon receives materials preferentially from the outer portions of the two bodies, likely leading to distinct refractory element and isotope compositions of the silicate Moon and Earth. The shaded zones on Theia and the proto-Earth show schematically the typical sampling regions for making the Moon, modified from Canup (2004). The color gradient shows an overall decreasing sampling probability toward planet interiors, namely the "shallow-province bias" (Warren, 2005). In the lower panel, the complete chemical and isotopic mixing predicted by the high-energy giant-impact hypothesis (Earth-Moon Synestia) (Lock et al., 2018) requires identical refractory element and mass-dependent isotope compositions of the BSM, LMO, and BSE.

refractory element compositions predicted for these giant-impact hypotheses, the bulk refractory element enrichment of the silicate Moon provides crucial and, possibly, decisive answers to how the Earth-Moon system formed.

To date, the refractory element enrichment of the Moon has been subject of markedly controversial assumptions. In previous studies, the initial lunar magma ocean (LMO) refractory trace element enrichment has been deemed to be substantially higher than the Earth (~4–5 times CI chondrite) (e.g., Snyder et al., 1992; Taylor et al., 2006) compared to ~2.7 times CI chondrite for the Earth (McDonough and Sun, 1995). Earth-like compositions (e.g., Warren, 2005; Taylor and Wieczorek, 2014, Lock et al., 2018) and enrichments as low as the CI chondrite (Rapp and Draper, 2018; Ji and Dygert, 2023) have also been used. Aside from these controversies, the importance of whether these trace element enrichment assumptions are consistent with the lunar major element constraints (Ca, Al, and Ti) has not been adequately explored in the literature. These disparate lunar trace element hypotheses await a clear quantitative resolution to be evaluated together with the major element constraints.

Much of the existing evidence for the BSM refractory element enrichment comes from extrapolating lunar surface refractory element abundances (Th and Al) into deeper mantle using mass-balance calculation to estimate the BSM enrichment (e.g., Taylor et al., 2006; Warren, 2005; Taylor and Wieczorek, 2014). However, the robustness and accuracy of these results are limited by our ability of determining the element concentration of the lunar crust and mantle (Warren, 2005; Taylor and Wieczorek, 2014). Additionally, the conclusions for other refractory elements of the Moon are limited by the few numbers of refractory elements that have already been directly investigated (Th and Al) (Warren, 2005; Taylor et al., 2006; Taylor and Wieczorek, 2014). Another approach used by O'Neill (1991) estimates the BSM element composition by mixing hypothetical mantle reservoirs from the impactor and the proto-Earth in certain proportions. However, this method is tied to the specific mixing proportion of Theia and the proto-Earth selected in the study (20 % vs. 80 %) and the requirement of Theia as an undifferentiated chondritic body (O'Neill, 1991), which was later realized to be likely a differentiated body in giant-impact models to meet the Moon's iron-depletion signature (e.g., Canup et al., 2023).

To circumvent these limitations, we developed a novel back-calculation methodology to enable determination of the initial refractory lithophile trace element abundances of the Moon (for 14 elements including Sr, Nb, and REEs), independent from the major element constraints. To achieve this objective, we utilize the trace element data of the direct products derived from the lunar magma ocean (LMO) and modeling of the element evolution of the LMO crystallization. Specifically, the plagioclase trace element compositions reported for 11 pristine Apollo ferroan anorthosites (FANs) (Pernet-Fisher et al., 2019) were selected. Their compositions chiefly preserve those of the LMO primary floatation cumulates in the late stage, with minimal mixing with other magmatic sources such as mare (<5 %) and KREEP (<1 %) [highly enriched in potassium (K), REEs, and phosphorus (P)] magmas (Pernet-Fisher et al., 2019). We also present an Eu vs. Sr diagram (Fig. S1) that shows the 11 pristine FAN plagioclase samples used in our study experienced negligible mixing with the KREEP or mare magma and record primarily the element compositions acquired from the LMO differentiation.

2. Methods

We examine a broad range of LMO crystallization models for a comprehensive test of the lunar trace element compositions. These models encompass LMO crystallization mineral sequences obtained from experiments and thermodynamic phase-equilibrium calculations, various BSM major element compositions [including Lunar Primitive Upper Mantle (LPUM) (Longhi, 2006), Taylor Whole Moon (TWM) (Taylor, 1982), and other modified versions], pure fractionation crystallization models, hybrid equilibrium-fractional crystallization models, and different assumptions of the initial LMO depth (ranging from ~600 km deep to the whole-Moon magma ocean) (Snyder et al., 1992; Elkins-Tanton et al., 2011; Lin et al., 2016; Rapp and Draper, 2018; Schmidt and Kraettli, 2022; Charlier et al., 2018; Johnson et al., 2021). We forward model the element-ratio evolution of the residual LMO liquids and flotation cumulates for different LMO crystallization models starting from a common near-chondritic LMO initial refractory element ratio (Supplementary Material: Section 3 and Table S3) using the compiled mineral-melt partition coefficients (Supplementary Material: Section 2 and Table S2).

A common feature of these LMO models is that as the LMO evolves to produce anorthosite by flotation, Eu and Sr become less incompatible in the LMO liquids and create increasing negative Eu anomaly (Eu/Eu*) and higher incompatible element/Sr ratio [such as $La/Sr_{(N)}$ and $Dy/Sr_{(N)}$, (*N*) denotes CI chondrite-normalized (Anders and Grevesse, 1989)] in both LMO residual liquids and flotation cumulates. Therefore, comparison of the observed highly fractionated trace element ratios (Eu/Eu*, $La/Sr_{(N)}$, and $Dy/Sr_{(N)}$) of the plagioclase samples with the calculated element ratio evolution of the flotation cumulates can yield sensitive estimates of the samples' degrees of crystallization during the LMO solidification. The selection of both $La/Sr_{(N)}$ and $Dy/Sr_{(N)}$ is meant to obtain constraints from both the light and heavy rare earth elements to test their consistency. Such data-model comparisons are similarly performed for the various LMO crystallization models. The critical advantage of using element-ratio comparison (rather than element-concentration comparison) to determine samples' degrees of crystallization is that the results are only dependent on the assumption of the initial LMO refractory element ratios, which are chondritic for all LMO models. As such, the determination is fully independent from the yet known, variously assumed initial LMO refractory element concentrations.

3. Results and discussion

3.1. Degree of LMO crystallization of lunar anorthosites

Fig. 2A shows the refractory element data of lunar samples compared to the forward modeling of the LMO element evolution starting from a BSE element enrichment (chondritic ratios and a uniform enrichment of ~2.7 times CI chondrites) (McDonough and Sun, 1995) under the Rapp and Draper (2018) LMO model. There is an excellent agreement for most elements. The exceptions are Cr (moderately-refractory) and Rb (moderately volatile), the latter of which is ~1/4 of BSE based on studies of Rb/Sr ratios (Borg et al., 2022). Fig. 2B highlights the element ratio comparison ($La/Sr_{(N)}$ and $Gd/Sr_{(N)}$ vs. Eu/Eu*) of the lunar data with the LMO residual liquid and the flotation cumulates (Supplementary Material: Section 3). Comparison between the lunar data and modeling results of other LMO models are presented in Fig. S4–S11.

Besides showing the element data of the plagioclase in pristine anorthosites (Pernet-Fisher et al., 2019), we also present the data for High-K KREEP (Warren, 1989) and lunar soils collected from the Apollo 14 and 16 missions (measured in this study) to test model consistency (Fig. 2B). The Apollo 14 soils reflect mostly the KREEP composition, and the Apollo 16 soils are thought to be the mixtures of the Procellarum KREEP Terrane and the Feldspathic Highland Terrane (Jolliff et al., 1999). These components provide additional independent tests for the modeled element-ratio evolution tied with individual LMO crystallization models.

Except for the phase-equilibrium TWM model of Johnson et al. (2021) (where garnet may be a stable phase in deep lunar mantle) and experimental "wet" shallow-LMO models (Lin et al., 2016) (Fig. S4 & S5), all other LMO crystallization models show a great match between the modeled flotation cumulate evolution and the plagioclase analyses of the pristine anorthosites. This agreement demonstrates their likely origin as products of late-stage LMO differentiation (Fig. 2 &

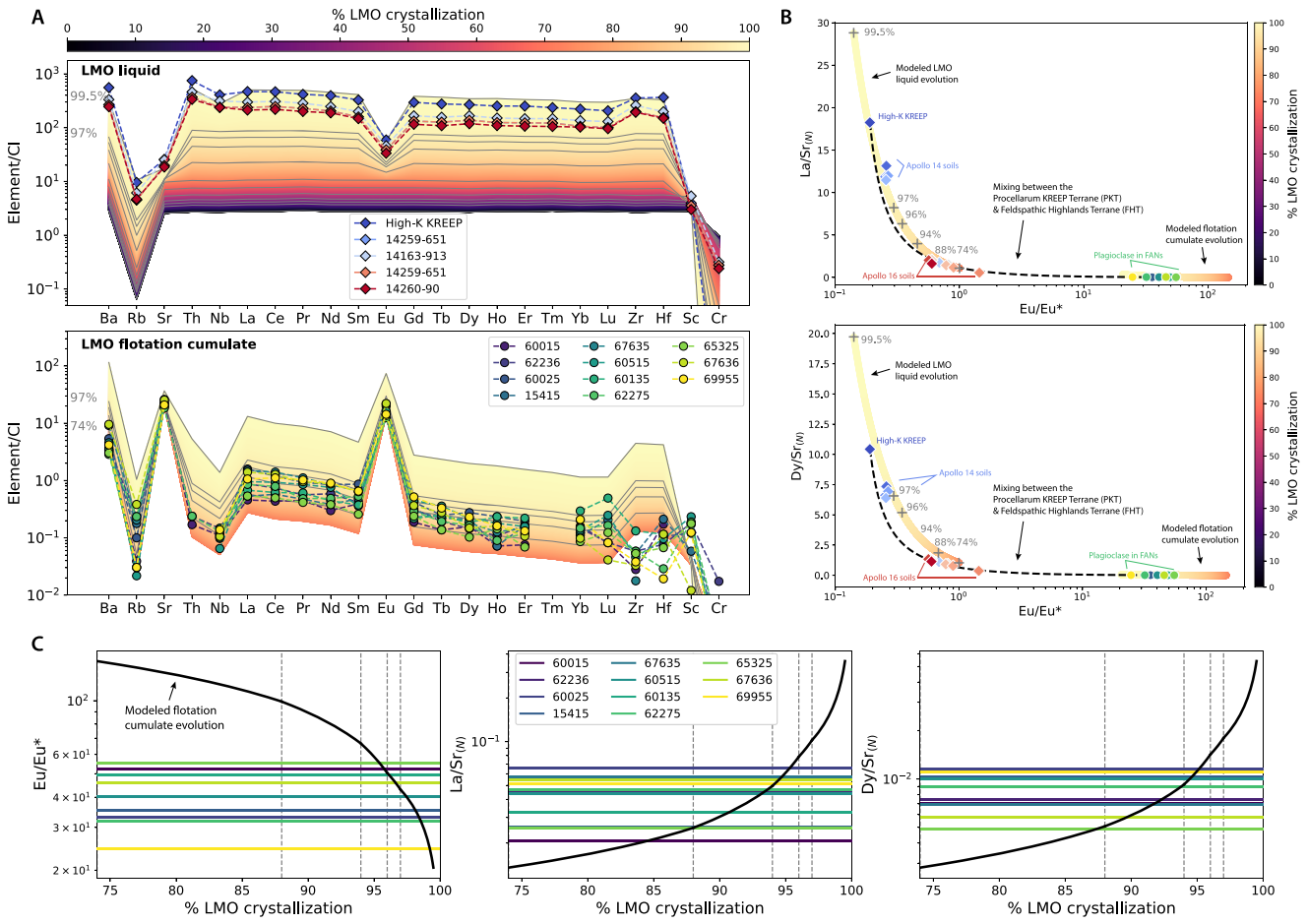

Fig. 2. Element ratio comparison between lunar data and LMO crystallization modeling for the Rapp and Draper (2018) model. (A) Trace element comparison between the LMO modeling (assuming an initial chondritic element ratio with Earth-like concentrations) and lunar data (High-K KREEP, Apollo 14 soils, and plagioclase in pristine FAN samples). Modeling results for the LMO liquid and flotation cumulates are color-coded as fields and delineated by fine grey lines and label markers. (B) Lunar trace element ratio data (symbols) compared with modeled evolution of the LMO liquid and floatation cumulates (curves) since 74 % LMO crystallization. The Apollo soil data (diamond symbols) are from this study and the FAN plagioclase data (circle symbols) are from (Pernet-Fisher et al., 2019). The modeled evolution curves are color-coded according to the % LMO crystallization, also labeled on the curves. The black dashed mixing curves were calculated assuming mixing between the High-K KREEP and a relatively primitive FAN sample 65325. (C) Comparison between the element ratios of the anorthosite plagioclase samples and the modeled flotation cumulate evolution. The average result from the three proxies gives the mean and two standard errors (2SEs) of the degree of crystallization of each plagioclase sample.

Fig. S6–11). Also, the modeled LMO liquid element-ratio evolution is consistent with the KREEP data (High-K KREEP and Apollo 14 soils) at extremely high degrees of LMO crystallization (~98–99.5 %) (Fig. 2B). Furthermore, the results of Apollo 16 soils are finely reproduced by the mixing curves between the High-K KREEP and a relatively primitive plagioclase component (FAN sample 65325) (Fig. 2B).

The inconsistency between the modeling results of the Johnson et al. (2021) and Lin et al. (2016) models and the lunar data is due to the models' significantly lower abundances of plagioclase in the late-stage crystallization sequences, which are too low to reproduce measurements such as the prominent negative Eu/Eu* signature of the KREEP (Fig. S4 & S5). For the other LMO crystallization models, the good agreement between the modeling results and the lunar data allows for determining the plagioclase samples' degree of crystallization using the three pairs of element ratios (Eu/Eu*, $La/Sr_{(N)}$, and $Dy/Sr_{(N)}$), each as an independent proxy (Fig. 2C). The average result from the three proxies gives the mean and two standard errors (2SEs) of the degree of crystallization of each plagioclase sample, determined from the individual LMO crystallization models (Table S4). The small uncertainties of most calculated mean degrees of crystallization (2SEs < 5 %) demonstrate the consistency of the three element-ratio proxies and the robustness of the results.

3.2. *Estimating the initial LMO refractory trace element concentrations*

We use the concentrations of Sr, Nb, and REEs (La, Ce, Pr, Nd, Sm, Eu, Gd, Tb, Dy, Ho, Er, Yb) of the anorthosite plagioclase, each as an independent element proxy, to compute the corresponding initial LMO refractory trace element concentrations. These 14 elements are selected because they are the ones measured best and completely for the FAN plagioclase samples (Fig. 2A). First, using the measured element concentrations of the plagioclase samples and mineral-melt partition coefficients, the element concentrations of the equilibrium parental magma of the plagioclase (LMO residual liquid) are computed (Fig. 3B, *Step 1*). Second, the calculated degree of crystallization of the plagioclase sample under a particular LMO crystallization model (Fig. 3A) is paired with these parental magma element compositions. Third, using the LMO element evolution calculation, we back-calculate to solve for the initial LMO element concentrations for the 14 elements (Fig. 3B, *Step 2*) (Supplementary Material: Section 5). Fourth, the average of these 14 elements gives the mean and 2SEs of the LMO initial refractory element enrichment inferred from this plagioclase sample. This calculation is performed for all the 11 plagioclase samples, whose least-squares-weighted average (considering their 2SEs) estimates the LMO initial refractory element enrichment under a particular LMO crystallization

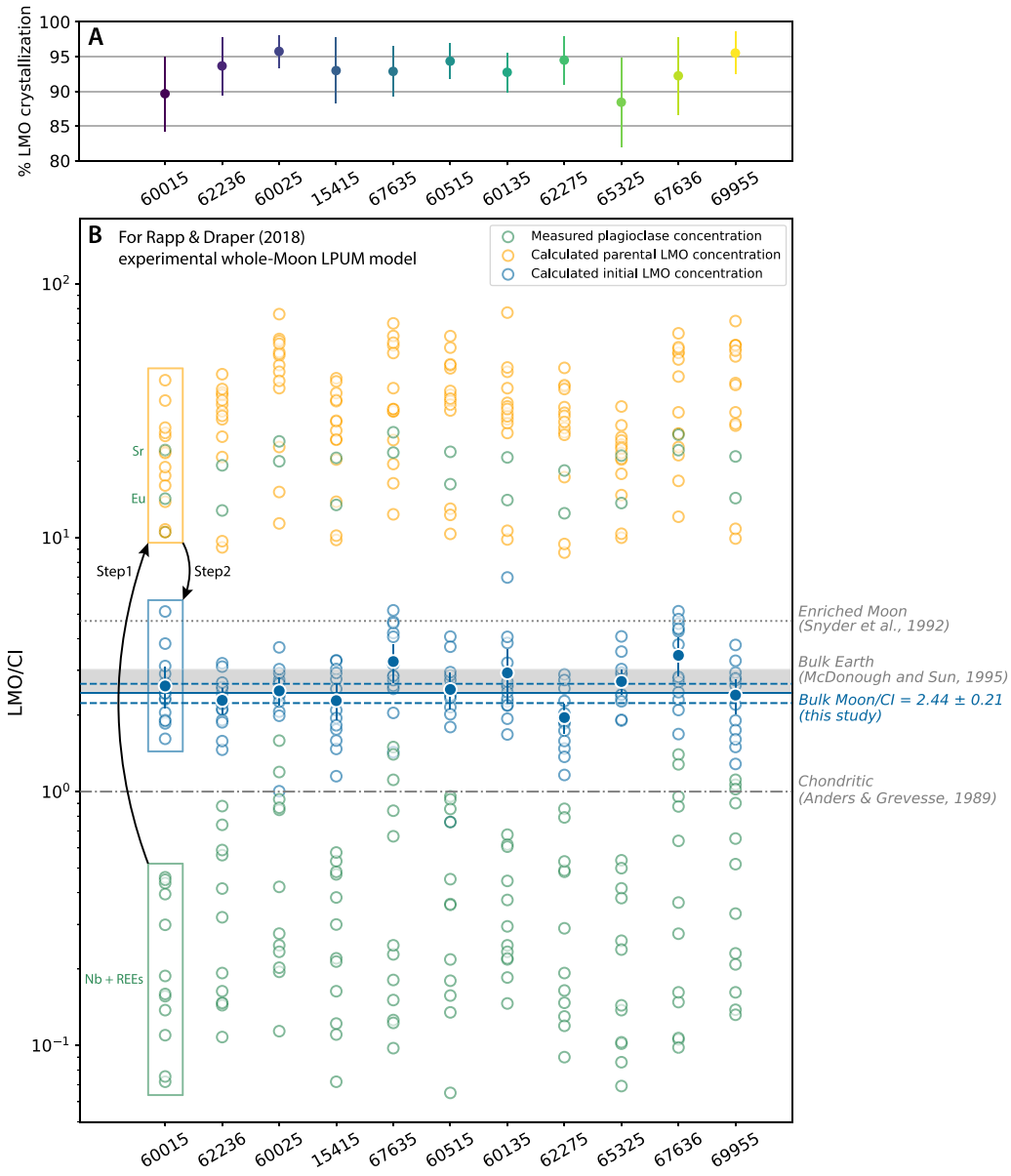

Fig. 3. Calculating the initial LMO trace element concentrations using the Rapp and Draper (2018) LMO model. **(A)** Results of degrees of LMO crystallization calculated for the anorthosite samples. **(B)** Calculation for the initial LMO trace element concentrations (Sr, Nb, and REEs). Step 1 shows converting the measured plagioclase element concentrations (green open circles) to their equilibrium parental LMO compositions (orange open circles). Step 2 represents back-calculating the initial LMO element concentration (blue open circles) using the parental LMO compositions and the corresponding degree of LMO crystallization (Fig. 3A). The average of all elements for one plagioclase sample gives an independent estimate of the mean and 2SEs of the LMO initial refractory trace element (blue solid circle with error bars). Weighted-least-squares averaging all estimates obtained from the 11 plagioclase samples yields the mean and 2SEs (the solid and dashed blue lines) of the LMO/CI refractory element enrichment (2.44 ± 0.21 times CI chondrite). In this case of Rapp and Draper (2018) experimental whole-Moon LMO model, the LMO initial concentration is equivalent to that of the BSM. The BSM enrichment is indistinguishable from the BSE enrichment (2.75 ± 0.28 times CI chondrite) shown as the gray horizontal envelope, whose relative uncertainty is estimated to be ~10 % (McDonough and Sun, 1995).

model. The calculation flow for the Rapp and Draper (2018) LMO model is exampled in Fig. 3. The results including other LMO crystallization models are provided in Fig. S12–S17.

The LMO models of Schmidt and Kraettli (2022), Rapp and Draper (2018), Johnson et al. (2021) are based on the whole-Moon magma ocean hypothesis. The model from Elkins-Tanton et al. (2011) prescribes a 1000-km deep initial LMO, similar to the whole-Moon coverage. For these models, our calculated LMO initial refractory element enrichment is equivalent to that of the bulk silicate Moon. The Charlier et al. (2018) and Lin et al. (2016) models were experimented according to an initially undifferentiated shallow-LMO assumption (~600 km), below which is an undifferentiated lunar deep mantle that shares the same bulk element composition as the LMO. Therefore, in these two shallow-LMO cases, the calculated LMO initial refractory element concentration is also equal to that of the bulk silicate Moon. The only exception is the Snyder et al. (1992) model that parameterizes an already enriched shallow-LMO to be the bulk composition (a residual shallow LMO after olivine separation to form deep mantle cumulates). Therefore, our calculated LMO initial refractory element composition for the Snyder et al. (1992) model estimates only this possibly enriched shallow LMO, which reflects an upper bound of the BSM enrichment (Fig. 4).

The determined LMO initial refractory trace element concentrations for the various LMO models span from 1.78 ± 0.18 to 3.12 ± 0.26 times CI chondrite (Fig. 4, x-axis data). Notably, three LMO models yield consistent trace element enrichments with the bulk silicate Earth (~2.75 ± 0.28 times CI chondrite), and the other four models give results

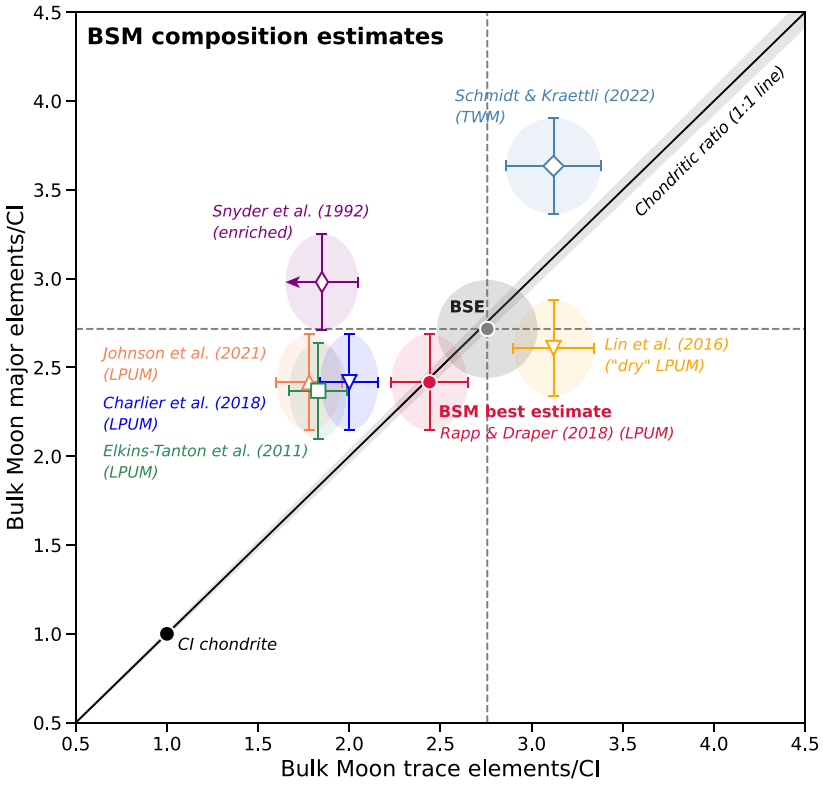

Fig. 4. Determining the refractory element compositions of the bulk silicate Moon. This diagram shows the cross-comparison of the calculated mean BSM refractory trace element enrichment (using Sr, Nb, and REEs) (this study) and the proposed mean major element enrichment (Ca and Al) for individual LMO crystallization models. The uncertainties on the x-axis are 2SEs determined from our calculation, and the error bars on the y-axis are assumed to be the same as that for the BSE (± 0.28 times CI chondrite, a ~10 % relative uncertainty) (McDonough and Sun, 1995). The 1:1 line shows the required relationship for a valid planetary composition with near-chondritic ratios of refractory elements. The shades of the 1:1 line represent an estimated 2 % maximum uncertainty in the refractory element ratios in the chondrite groups from the summary of Alexander (2019a) and Alexander (2019b). The only valid, self-consistent composition is obtained for the Rapp and Draper (2018) model, which defines the best-estimated BSM refractory element composition and is consistent with the BSE within uncertainty. An arrow pointing left on the error bar reflects that the estimated BSM enrichment is likely lower than the presented value.

between the silicate Earth and the chondritic abundances. None of the results are close to the hypothesized chondritic abundance or a highly enriched abundance (~4–5 times CI chondrite).

The observed difference in these trace element enrichment estimates is mainly caused by the different saturation stages and fractionating abundances of plagioclase in different LMO models. The highly fractionated element ratios (Eu/Eu*, $La/Sr_{(N)}$, and $Dy/Sr_{(N)}$) are sensitive to plagioclase crystallization effects. In the Johnson et al. (2021), Elkins-Tanton et al. (2011), Snyder et al. (1992), and Charlier et al. (2018) LMO models, plagioclase starts to saturate in the LMO in relatively late stages (after ~78 % LMO crystallization) compared to the Lin et al. (2016), Schmidt and Kraettli (2022), and Rapp and Draper (2018) models, in which plagioclase crystallization starts at ~70 % of LMO crystallization. Therefore, the estimated degrees of crystallization for the plagioclase samples in the former four models are systematically higher than those obtained for the latter three models. This factor further leads to the systematic difference in the back-calculated LMO initial refractory concentrations between the two groups of models.

3.3. Comparison of major and trace element constraints for the bulk Moon: implications for a thoroughly-mixed Moon-forming disk

These discrepant trace element estimates from different LMO models cannot be used solely to affirm the BSM enrichment. However, the independent trace element estimates gain increasing constraining power after combining with estimates for the BSM refractory major element concentrations. For any set of estimates, the consistency between the LMO refractory trace element (Sr, Nb, REEs) and major element (i.e., Al, Ca) enrichments needs to be first verified to test the qualification as a self-consistent model.

We plot the LMO refractory trace element estimates (from our study) versus the major element enrichments used for individual LMO crystallization models in Fig 4. The y-axis data show the mean of Al and Ca enrichments of the bulk composition assumed in each LMO crystallization model. Except for the Schmidt and Kraettli (2022) and Snyder et al. (1992) models that assume more refractory-element-enriched BSM major element compositions, the other five models all assume a BSM major element composition essentially identical to the BSE (LPUM) (Longhi, 2006). We find that the BSM refractory major and trace element compositions determined for the Rapp and Draper (2018) model form the only self-consistent composition, whose means are consistent with the 1:1 relationship within uncertainty and define the best estimate for the BSM element composition. The other models exhibit moderately inconsistent major and trace element estimates, but their estimates cluster around the BSE composition (Fig. 4). We underscore the importance of examining major and trace elements together to verify internal coherency of the proposed LMO models before further interpretations, a critical step forward toward establishing the accurate lunar composition.

The self-consistent refractory major and trace element enrichments obtained for the Rapp and Draper (2018) model is based on an initial whole-Moon magma ocean, whose refractory element composition reflects that of the BSM. An initially fully molten Moon has also been independently supported by increasingly converging geophysical and geochemical evidence from recent studies (Canup et al., 2015; Lock et al., 2018; Steenstra et al., 2020; Canup et al., 2023; Schmidt and

Kraettli, 2022). The resolved BSM refractory element enrichment agrees with the BSE values within uncertainty (BSM/BSE = 0.89 ± 0.12) (Fig. 4), consistent with other estimates for Th and Al using a different mass-balance method (Warren, 2005; Taylor and Wieczorek, 2014).

The observed near-identical BSM and BSE refractory lithophile elemental ratio and enrichment is a distinctive feature predicted by the high-energy giant-impact (Synestia) model (Lock et al., 2018) due to vigorous mixing of the Moon-forming disk in a homogenized silicate fluid. This marked refractory element similarity is at odds with the poor mixing conditions of the canonical giant-impact models. Its compatibility with other Moon-forming models that claim better disk mixing has yet to be quantitatively tested (e.g., Pahlevan and Stevenson, 2007; Charnoz and Michaut, 2015; Gammie et al., 2016). Along with the isotopic similarities between the Earth and Moon (e.g., Zhang et al., 2012; Wang et al., 2015; Young et al. 2016; Sossi and Moynier, 2017; Poitrasson et al., 2019; Sedaghatpour and Jacobsen, 2019; Fischer et al., 2021; Fu et al., 2023), our new result means that the silicate portions of the Earth and the Moon are essentially identical in both chemistry and isotopic composition, except for the more volatile elements. This finding places further constraints on a likely high-energy giant-impact origin of the Earth-Moon system, in which a fully molten Moon formed in a well-mixed protolunar disk of BSE composition, as hypothesized and permitted by models like the Earth-Moon Synestia (Lock et al., 2018).

The only silicate Earth-Moon compositional differences are the Moon's relative depletion in more volatile elements (e.g., Taylor and Wieczorek, 2014; Lock et al., 2018; Charnoz et al., 2021; Solomatova and Caracas, 2023) and the distinct moderately-volatile-element isotope compositions, such as K, Zn, Rb, and Sn (Wang and Jacobsen, 2016; Wang et al., 2019; Dauphas et al., 2022; Nie and Dauphas, 2019; Canup et al., 2015). Both exceptions were sought to be explained quantitatively in the Synestia and other protolunar disk models (Canup et al., 2015; Lock et al., 2018; Charnoz et al., 2021; Dauphas et al., 2022). In comparison, regarding the more refractory elements, reproducing the Moon's low iron content remains the central consideration of most geophysical models (Canup et al., 2023), while verifying if such geophysical models can also reproduce other refractory element (isotopic) observations has received far less attention and quantitative investigation. Except for the Synestia model (Lock et al., 2018), substantial verification of the Earth-Moon refractory element composition in other existing giant-impact physical models remains scarce, yet it opens fresh windows for harnessing this critical element array. We propose that an increasing endeavor in quantifying the predicted Earth-Moon refractory chemical and isotopic consequences tied to various giant-impact physical models would shed essential new light into successfully testing the Moon-formation theories.

4. Conclusions

We developed a new methodology to constrain the refractory element composition of the BSM, a fundamental property of the Moon subject to notable controversies. By combining the chemical compositions of the pristine lunar anorthosite samples and modeling the LMO crystallization chemical evolution, we have determined the initial refractory trace element compositions in the LMO tied to various LMO models. The self-consistent set of refractory major and trace element enrichments yields the best estimate for the BSM refractory element composition, which agrees with the BSE composition within uncertainty. This striking Earth-Moon refractory element similarity is a distinctive feature predicted by the high-energy, high-angular-momentum giant-impact hypothesis (Synestia), with an initially fully molten Moon formed in a rigorously mixed disk of BSE-composition fluid. Such a similarity is difficult to be explained by the canonical low-energy giant-impact models due to poor mixing of the impactor and the proto-Earth. Its compatibility with other proposed disk equilibration models that claim better disk mixing needs to be rigorously verified in future studies. Our findings provide further evidence that forming the Earth-Moon system requires a thoroughly-mixed protolunar disk of chemical and isotopic homogenization, likely enabled by a high-energy giant impact proposed in emerging models like the Synestia.

CRediT authorship contribution statement

Hairuo Fu: Writing – review & editing, Writing – original draft, Visualization, Validation, Software, Resources, Methodology, Investigation, Formal analysis, Data curation, Conceptualization. **Stein B. Jacobsen:** Writing – review & editing, Validation, Supervision, Resources, Project administration, Methodology, Investigation, Formal analysis, Conceptualization.

Declaration of competing interest

The authors declare that they have no known competing financial interests or personal relationships that could have appeared to influence the work reported in this paper.

Data availability

The authors declare that the data supporting the findings of this study are available within the article and its Supplementary Material files.

Acknowledgments

We are grateful to G. Jeffrey Taylor and an anonymous reviewer for their constructive reviews of this work. We are thankful to Olivier Mousis for the careful editorial handling. This research was partly supported by the Department of Energy National Nuclear Security Administration under awards DE-NA0003904 and DE-NA0004084 (to S.B.J., principal investigator) with Harvard University and by the Sandia Z Fundamental Science Program. This research represents the authors' views and not those of the Department of Energy.

Supplementary materials

Supplementary material associated with this article can be found, in the online version, at doi:10.1016/j.epsl.2024.119008.

References

Alexander, C.M., 2019a. Quantitative models for the elemental and isotopic fractionations in the chondrites: the non-carbonaceous chondrites. Geochim. Cosmochim. Acta 254, 246–276.
Alexander, C.M., 2019b. Quantitative models for the elemental and isotopic fractionations in chondrites: the carbonaceous chondrites. Geochim. Cosmochim. Acta 254, 277–309.
Anders, E., Grevesse, N., 1989. Abundances of the elements: meteoritic and solar. Geochim. Cosmochim. Acta 53, 197–214.
Borg, L.E., Brennecka, G.A., Kruijer, T.S., 2022. The origin of volatile elements in the Earth–Moon system. Proc. Natl. Acad. Sci. 119.
Canup, R.M., 2004. Simulations of a late lunar-forming impact. Icarus 168, 433–456.
Canup, R.M., 2012. Forming a Moon with an Earth-like composition via a giant impact. Science 338, 1052–1055.
Canup, R.M., Visscher, C., Salmon, J., Fegley, B., 2015. Lunar volatile depletion due to incomplete accretion within an impact-generated disk. Nat. Geosci. 8, 918–921.
Canup, R.M., Righter, K., Dauphas, N., Pahlevan, K., Ćuk, M., Lock, S.J., et al., 2023. Origin of the Moon. Rev. Mineral. Geochem. 89 (1), 53–102.
Charlier, B., Grove, T.L., Namur, O., Holtz, F., 2018. Crystallization of the lunar magma ocean and the primordial mantle-crust differentiation of the Moon. Geochim. Cosmochim. Acta 234, 50–69.
Charnoz, C., Michaut, C., 2015. Evolution of the protolunar disk: dynamics, cooling timescale and implantation of volatiles onto the Earth. Icarus 260, 440–463 (2015).
Charnoz, S., Sossi, P.A., Lee, Y., Siebert, J., Hyodo, R., Allibert, L., Pignatale, F.C., Landeau, M., Oza, A., Moynier, F., 2021. Tidal pull of the Earth strips the proto-Moon of its volatiles. Icarus 364, 114451.
Dauphas, N., Nie, N.X., Blanchard, M., Zhang, Z.J., Zeng, H., Hu, J.Y., Méheut, M., Visscher, C., Canup, R.M., Hopp, T., 2022. The extent, nature, and origin of K and Rb

depletions and isotopic fractionations in Earth, the Moon, and other planetary bodies. Planet. Sci. J. 3.
Elkins-Tanton, L.T., Burgess, S., Yin, Q.Z., 2011. The lunar magma ocean: reconciling the solidification process with lunar petrology and geochronology. Earth Planet Sci. Lett. 304, 326–336.
Elkins-Tanton, L.T., 2012. Magma oceans in the inner solar system. Annu. Rev. Earth Planet Sci. 40, 113–139.
Fischer, R.A., Zube, N.G., Nimmo, F., 2021. The origin of the Moon's Earth-like tungsten isotopic composition from dynamical and geochemical modeling. Nat. Commun. 12.
Fu, H., Jacobsen, S.B., Sedaghatpour, F., 2023. Moon's high-energy giant-impact origin and differentiation timeline inferred from Ca and Mg stable isotopes. Commun. Earth Environ. 4, 307.
Gammie, C.F., Liao, W., Ricker, P.M., 2016. A hot big bang theory: magnetic fields and the early evolution of the protolunar disk. Astrophys. J. 828.
Hosono, N., Karato, S., Makino, J., Saitoh, T.R., 2019. Terrestrial magma ocean origin of the Moon. Nat. Geosci. 12, 418–423.
Jolliff, B.L., Gillis, J.J., Haskin, L.A., Korotev, R.L., Wieczorek, M.A., 1999. Major lunar crustal terranes: surface expressions and crust-mantle origins. J. Geophys. Res. 105, 4197–4216.
Ji, D., Dygert, N., 2023. Trace element evidence for serial processing of the lunar flotation crust and a depleted bulk Moon. Earth Planet Sci. Lett. 602, 117958.
Johnson, T.E., Morrissey, L.J., Nemchin, A.A., Gardiner, N.J., Snape, J.F., 2021. The phases of the Moon: modelling crystallisation of the lunar magma ocean through equilibrium thermodynamics. Earth Planet. Sci. Lett. 556, 116721.
Kegerreis, J.A., Ruiz-Bonilla, S., Eke, V.R., Massey, R., Sandnes, T., Teodoro, L., 2022. Immediate origin of the Moon as a Post-impact satellite. ApJL 937.
Lin, Y., Tronche, E.J., Steenstra, E.S., van Westrenen, W., 2016. Evidence for an early wet Moon from experimental crystallization of the lunar magma ocean. Nat. Geosci. 10, 1-1.
Lock, S.J., Stewart, S.T., Petaev, M.I., Leinhardt, Z., Mace, M.T., Jacobsen, S.B., Ćuk, M., 2018. The origin of the Moon within a terrestrial synestia. J. Geophys. Res.: Planets 123, 910–951.
Longhi, J., 2006. Petrogenesis of picritic mare magmas: constraints on the extent of early lunar differentiation. Geochim. Cosmochim. Acta 70, 5919–5934.
Melosh, H.J., 2014. New approaches to the Moon's isotopic crisis. Philosoph. Trans. R. Soc. A: Math. Phys. Eng. Sci. 372.
McDonough, W.F., Sun, S.S., 1995. The composition of the Earth. Chem. Geol. 120, 223–253.
Mougel, B., Moynier, F., Gopel, C., 2018. Chromium isotopic homogeneity between the Moon, the Earth, and enstatite chondrites. Earth Planet. Sci. Lett. 481, 1–8.
Nie, N.X., Dauphas, N., 2019. Vapor drainage in the protolunar disk as the cause for the depletion in volatile elements of the Moon. Astrophys. J. Lett. 884.
O'Neill, H.S., 1991. The origin of the moon and the early history of the earth—A chemical model. Part 1: the moon. Geochim. Cosmochim. Acta 55, 1135–1157.
Pahlevan, K., Stevenson, D.J., 2007. Equilibration in the aftermath of the lunar-forming giant impact. Earth Planet Sci. Lett. 262, 438–449.
Pernet-Fisher, J.F., Deloule, E., Joy, K.H., 2019. Evidence of chemical heterogeneity within lunar anorthosite parental magmas. Geochim. Cosmochim. Acta 266, 109–130.
Poitrasson, F., Zambardi, T., Magna, T., Neal, C.R., 2019. A reassessment of the iron isotope composition of the Moon and its implications for the accretion and differentiation of terrestrial planets. Geochim. Cosmochim. Acta 267, 257–274.
Qin, L., Alexander, C.M., Carlson, R.W., Horan, M.F., Yokoyama, T., 2010. Contributors to chromium isotope variation of meteorites. Geochim. Cosmochim. Acta 74, 1122–1145.
Rapp, J.F., Draper, D.S., 2018. Fractional crystallization of the lunar magma ocean: updating the dominant paradigm. Meteorit. Planet Sci. 53, 1432–1455.
Schmidt, M.W., Kraettli, G., 2022. Experimental crystallization of the lunar magma ocean, initial selenotherm and density stratification, and implications for crust formation, overturn and the bulk silicate moon composition. J. Geophys. Res.: Planets 127.
Sedaghatpour, F., Jacobsen, S.B., 2019. Magnesium stable isotopes support the lunar magma ocean cumulate remelting model for mare basalts. Proc. Natl. Acad. Sci. 116, 73–78.
Snyder, G.A., Taylor, A., Neal, C.R., 1992. A chemical model for generating the sources of mare basalts: combined equilibrium and fractional crystallization of the lunar magmasphere. Geochim. Cosmochim. Acta 56, 3809–3823.
Solomatova, N.V., Caracas, R., 2023. Earth's volatile depletion trend is consistent with a high-energy Moon-forming impact. Commun. Earth Environ. 4.
Sossi, P.A., Moynier, F., 2017. Chemical and isotopic kinship of iron in the Earth and Moon deduced from the lunar Mg-Suite. Earth Planet Sci. Lett. 471, 125–135.
Steenstra, E.S., Berndt, J., Klemme, S., Fei, Y., van Westrenen, W., 2020. A possible high-temperature origin of the Moon and its geochemical consequences. Earth Planet Sci. Lett. 538, 116222.
Taylor, G.J., Wieczorek, M.A., 2014. Lunar bulk chemical composition: a post-gravity recovery and interior laboratory reassessment. Philosoph. Trans. R. Soc. A: Math. Phys. Eng. Sci. 372.
Taylor, S.R., 1982. Planetary Science: A Lunar Perspective. Lunar and Planetary Institute, Houston, p. 502.
Taylor, S.R., Taylor, G.J., Taylor, L.A., 2006. The Moon: a Taylor perspective. Geochim. Cosmochim. Acta 70, 5904–5918.
Warren, P.H., 1989. KREEP: major-element diversity, trace-element uniformity (almost). In: Taylor, G.J., Warren, P.H. (Eds.), Workshop On Moon in Transition: Apollo 14, KREEP, and Evolved Lunar Rocks. Lunar and Planetary Institute, Houston, Texas, pp. 149–153.
Warren, P.H., 2005. New' lunar meteorites: implications for composition of the global lunar surface, lunar crust, and the bulk Moon. Meteorit. Planet. Sci. 40, 477–506.
Wang, K., Jacobsen, S.B., Sedaghatpour, F., Chen, H., Korotev, R.L., 2015. The earliest lunar magma ocean differentiation recorded in Fe isotopes. Earth Planet Sci. Lett. 430, 202–208.
Wang, X., Fitoussi, C., Bourdon, B., Fegley, B., Charnoz, S., 2019. Tin isotopes indicative of liquid–vapour equilibration and separation in the Moon-forming disk. Nat. Geosci. 12, 707–711.
Wang, K., Jacobsen, S.B., 2016. Potassium isotopic evidence for a high-energy giant impact origin of the Moon. Nature 538, 487–490.
Young, E.D., Kohl, I.E., Warren, P.H., Rubie, D.C., Jacobson, S.A., Morbidelli, A., 2016. Oxygen isotopic evidence for vigorous mixing during the Moon-forming giant impact. Science 351, 493–496.
Zhang, J., Dauphas, N., Davis, A.M., Leya, I., Fedkin, A.V., 2012. The proto-Earth as a significant source of lunar material. Nat. Geosci. 5, 251–255.
Zindler, A., Jacobsen, S.B., 2010. Rethinking lunar formation: back to the future?. In: *Proc. 41st Lunar Planet. Sci. Conf.* Abstract No. 2702. Lunar and Planetary Institute.